Gas-phase mass-transfer resistance at PEMFC electrodes
Part 1. Diffusive and forced migration through a porous medium

E. Arato *, P. Costa

*Department of Environmental Engineering, DIAM, University of Genoa,
via Opera Pia 15, 16145 Genoa, Italy*

Abstract

The mass-transfer phenomena at the electrodes and, in particular, the diffusion of oxygen at the cathode significantly affect the limit performance of PEMFCs. Some particular geometric arrangements, such as the interdigitated or serpentine, have demonstrated their effectiveness in lowering diffusive resistances.

It is possible to have a better understanding of these phenomena by determining the various possible diffusive regimes taking place inside the porous layer close to the electrodes. In each regime the interaction between diffusive and forced flows can be expressed in terms of Peclet numbers and the overall diffusive resistance in terms of Sherwood numbers.

In this way, the comparison of traditional and non-traditional geometric arrangements can be more deeply studied, so that the problems relating to the simulation and optimisation of the cell can be more efficiently dealt with.
© 2005 Elsevier B.V. All rights reserved.

Keywords: Transport phenomena; Modelling; Polymeric membrane fuel cells; Gas flow mode

.

1. Introduction

The full practical relevance of the transport phenomena occurring in polymeric membrane fuel cells (PEMFCs) is now almost universally acknowledged. First of all, the proton and water migration through the polymeric membrane, which determines the membrane polarisation, is sensitive to membrane hydration, so humidity control has become a central goal of PEMFC studies. These phenomena have been discussed elsewhere [1–8].

In this paper attention will be paid to the gas-phase mass transfer [6,9–13]. Some recent articles [14] have emphasised the role of diffusive phenomena occurring in polymeric membrane fuel cells: the mass transfer by diffusion at the electrodes and, in particular, the diffusion of oxygen at the cathode significantly affects the limit performance of the cell. Some new geometric arrangements for feeding the cell, such as interdigitated geometry, have demonstrated their effectiveness [2,14,15] in lowering diffusive resistance.

Even more recently [16], attention has been centred on similar results that can be obtained with serpentine geometry, so widening the range of the parameters to be taken into account in design and optimisation. In that work the discussion of the migration flows at the electrode was based on a simplified physical–mathematical description and its analytical solution and, for that purpose, a number of simplifying assumptions were used; many of those are widely acceptable and quite usual; others, a little less obvious or partially implicit, are still fully coherent in terms of a first approximation discussion. But, as is to be expected, the most delicate points concern an appropriate choice of the boundary conditions.

While other, more detailed investigations of the matter are certainly advisable, a better understanding of the role of mass-transfer phenomena is readily achievable, even now, by simply

* Corresponding author. Tel.: +39 010 3532926; fax: +39 010 3532589.
  E-mail address: betta@diam.unige.it (E. Arato).

considering the various possible diffusive regimes. In the following sections, the various limit regimes will be determined and the interaction of diffusive and forced flows for each regime will be expressed in terms of Peclet numbers and the overall diffusive resistance will be expressed in terms of Sherwood numbers, which are, in turn, functions of the Peclet number.

The results of this approach will then be used in the discussion of a number of experimental findings regarding traditional [7,17], interdigitated and serpentine [16] cells. A better understanding of the role of gas mass transfer will show its effectiveness in explaining some important differences in the performance of these cells, especially in terms of limit current. In such a way the comparison of traditional and non-traditional geometric arrangements and the related optimisation problems can be more clearly set out.

Successively, in the second part of this work, a comparison of interdigitated and serpentine geometries will be further developed by explicitly taking the pressure differences between contiguous channels and their dependence on the head losses through the channels into account.

2. A reference scheme

The spatial domain near the electrode surface considered here has a rectangular $h(b + d)$ section, where h on the x-axis is the thickness of the diffusion layer, d on the y-axis is the space between one channel and the next and b is the width of each adduction channel (see Fig. 1). Following Zhukovsky and Pozio, [16], the diffusion and migration phenomena in the partial hd domain can be described according to the differential equation

$$-\rho D \left(\frac{\delta^2 \omega}{\delta x^2} + \frac{\delta^2 \omega}{\delta y^2} \right) + \rho v \frac{\delta \omega}{\delta y} = 0, \quad 0 < y < d, \ 0 < x < h \tag{1}$$

In Eq. (1) the density ρ and the diffusivity D of the gas phase moving inside the porous medium are considered constant; the stagnant film effects are neglected, but the correspondent errors are surely less than 5%; a steady state can also be assumed, because of the diffusion times of the porous system, which are of the order of 1 s or less.

To describe the flow field, a uniform velocity v along the y-axis is considered. This simplification is rather obvious from many points of view, but it is certainly to some extent unrealistic at the boundaries ($y = 0$ and $y = d$), where the flow field has to join the external one.

It is evident that the portion of the porous medium corresponding to the channel (see Fig. 1) is not considered in determining the spatial domain. In such a way a fraction of the reagent reaching the electrode is forgotten and the total rate will be underestimated.

The boundary conditions associated with Eq. (1) are

$$x = 0, \quad \frac{\delta \omega}{\delta x} = 0 \tag{2}$$

$$x = h, \quad \omega = 0 \tag{3}$$

$$y = 0, \quad \omega = f_1(x), \quad f_1(0) = \omega_1 \tag{4}$$

$$y = d, \quad \omega = f_2(x), \quad f_2(0) = \omega_2 \tag{5}$$

Beside the obvious, and fully acceptable, assumption of an impermeable metallic surface at $x = 0$, it is also useful to assume an instantaneous reaction on the cathodic surface at $x = h$. This is the approach to define the reference behaviour in terms of limit current.
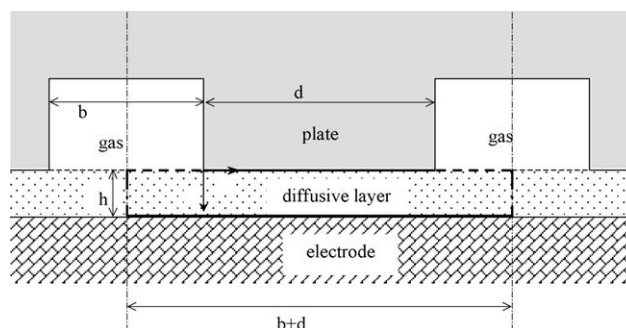

Fig. 1. The spatial domain considered.

The other two boundary conditions for $y = 0$ and $y = d$ correspond to the assumption of a reasonable composition profile through the layer. For a given f_1 and f_2 the solution of the system $\omega(x, y)$ can be obtained and the mean flux of the reagent (i.e. oxygen), which leaves the domain by reacting at the electrode, can be calculated as

$$N_{\mathrm{m}x,x=h} = \left(\frac{1}{d}\right) \int_0^d N_{x,x=h} \, \mathrm{d}y$$

$$= -\left(\frac{\rho D}{d}\right) \int_0^d \left(\frac{\delta \omega}{\delta x}\right)_{x=h} \mathrm{d}y \tag{6}$$

or as the sum of the fluxes entering the domain

$$N_{\mathrm{m}x,x=h} = \left(\frac{h}{d}\right) (N_{\mathrm{m}y,y=0} - N_{\mathrm{m}y,y=d})$$

$$= \left(\frac{1}{d}\right) \int_0^h (N_{y,y=0} - N_{y,y=d}) \, \mathrm{d}x$$

$$= -\left(\frac{\rho D}{d}\right) \int_0^h \left[\left[\left(\frac{\delta w}{\delta y}\right)\right]_{y=0} - \left(\frac{\delta \omega}{\delta y}\right)_{y=d}\right] \mathrm{d}x \tag{7}$$

When the functions f_1 and f_2 are specified as

$$y = 0, \quad \omega = \omega_1 \cos\left(\frac{\pi x}{2h}\right) \tag{4'}$$

$$y = d, \quad \omega = \omega_2 \cos\left(\frac{\pi x}{2h}\right) \tag{5'}$$

the system leads to the solution reported in [16].

In particular, for a negligible velocity v, that is a fully diffusive migration, we have

$$v = 0, \quad N_{\mathrm{m}x,x=h} = \left(\frac{\rho D}{d}\right)(\omega_1 + \omega_2)\mathrm{tgh}\left(\frac{\pi d}{4h}\right)$$

$$\approx \left(\frac{\rho D}{d}\right)(\omega_1 + \omega_2), \quad \frac{\pi d}{4h} > 3 \tag{8}$$

This solution is probably fairly accurate: the mass-transfer regime is completely diffusive, the mean driving force is $(\omega_1 + \omega_2)/2$ and the mean diffusion path is about $d/2$. However, a correction still has to be introduced to take into account the fraction of the reagent rate referring to the width b of the channel.

As the velocity v increases, the sinusoidal boundary conditions (4′) and (5′) become less realistic. For high velocities it appears more reasonable to make reference to a uniform profile along the x-axis at the beginning of the domain

$$y = 0, \quad x < h, \quad \omega = \omega_1 \tag{4''}$$

while the profile at the end ($y = d$) becomes quite insignificant.

In the light of the above discussion, there still appears to be a wide area for investigation by analytical or numerical methods. By using only a very simple approach, however, a preliminary and introductory, but reliable analysis of the whole problem is immediately available, making it possible to determine what kind of solution is to be expected for the various possible limit regimes.

3. Definition of the limit regimes

For the purpose of determining the limit regimes, it is useful to make reference to the following characteristic times. Two diffusion times are of interest, the axial diffusion time (along the y-axis)

$$t_{\mathrm{D}y} = \frac{d^2}{D} \tag{9}$$

and the transversal diffusion time (along the x-axis)

$$t_{\mathrm{D}x} = \frac{h^2}{D} \tag{10}$$

They have to be compared to the residence time inside the porous medium

$$t_{\mathrm{R}y} = \frac{d}{v} \tag{11}$$

so that the correlated dimensionless parameters, such as the axial Peclet number,

$$Pe\,y = \frac{t_{\mathrm{D}y}}{t_{\mathrm{R}y}} = d\frac{v}{D} \tag{12}$$

and the transversal Peclet number

$$Pe\,x = \frac{t_{\mathrm{D}x}}{t_{\mathrm{R}y}} = \frac{h^2 v}{dD} \tag{13}$$

can be defined.

When $d \gg h$, as can reasonably be assumed, $Pe\,x \ll Pe\,y$.

Besides the already cited diffusive regime, two others must be considered:

- R1:

$$Pe\,y \ll 1 \tag{14}$$

in which the flux of the reagent depends on the mean driving force and, then, on the conditions at both the beginning and the end of the spatial domain according to Eq. (8).

A forced regime must also be considered:

- R2:

$$Pe\,y \gg 1 \tag{15}$$

in which the effects of axial diffusion are negligible in comparison to the forced migration: the inlet composition at the beginning of the domain can be considered uniform along the x-axis, as explained in condition (4″), while the composition at the domain end loses importance.

Within the forced regime, two more sub-regimes can be considered; a flow-rate controlled regime and a pellicular-forced regime. In a flow-rate controlled regime

- R2.1:

$$Pe\,y \gg 1, \quad Pe\,x \ll 1 \tag{16}$$

the residence time is long enough to allow the diffusion of the entire reagent at the electrode. The flux to the electrode is then controlled by the forced flow rate entering the domain with a good approximation

$$N_{\mathrm{m}x,x=h} \approx \left(\rho v \frac{h}{d} \right) \omega_1 \tag{17}$$

and is directly proportional to the velocity. In a pellicular-forced regime

- R2.2:

$$Pe\, y \gg 1, \qquad Pe\, x \gg 1 \tag{18}$$

the residence time is much shorter than the transversal diffusion time, so that only the reagent of a thin pellicular layer near the electrode can be consumed. The flux and its mean value can be derived from the well-known formula [18] for transient diffusion on a semi-infinite layer

$$N_{\mathrm{m}x,x=h} \approx \rho \omega_1 \left(4D \frac{v}{\pi d} \right)^{1/2} \tag{19}$$

and now depends on the square root of the velocity.

In both the forced sub-regimes, where the migration flow field is much more important than the diffusion one, any description yielding a result independent of the velocity is obviously quite inadequate.

4. The Sherwood number

By introducing the reference flux

$$N_{\mathrm{r}} = \frac{\rho D_{\mathrm{M}} \omega_1}{b} \tag{20}$$

which corresponds to the diffusion in the homogeneous gas phase of a square section bb of the channel; the ratio of the calculated flux and the reference flux defines the Sherwood number we have used in a number of works on the simulation of PEMFCs for different geometries [2,14]. For a full analysis, the entire electrode surface has to be considered in the definition of the actual mean flux if it is to be compared to the reference flux: so, apart from the mean flux referring to the length d ($N_{\mathrm{m}x,\,x=h}$), allowance must also be made for the mean flux referring to the length b ($N'_{\mathrm{m}x,\,x=h}$), giving

$$Sh = \frac{dN_{\mathrm{m}x,x=h} + bN'_{\mathrm{m}x,x=h}}{(d+b)N_{\mathrm{r}}} \tag{21}$$

In such a way, a Sherwood number of the order of unity should be obtained if the homogeneous mass transfer in the channels is controlling, and $Sh \ll 1$ is obtained when the diffusion in the porous medium is controlling; the effect of a forced-flow field can further increase the Sherwood number to some unities or more.

Making reference to a single-channel configuration in the diffusive regime, assuming the result of (8), and adding a reasonable estimation for the fraction of the reagent rate referring to the width b of a square channel (homogeneous diffusion on

a $b/2$ mean path in series with heterogeneous diffusion on an h path) we have

$$N'_{\mathrm{m}x,x=h} \approx \frac{(\rho D)(\omega_1 + \omega_2)}{h + bD/(2D_{\mathrm{M}})} \tag{22}$$

In such instances values of Sh can be obtained

$$Sh \approx \left[\frac{\omega_1 + \omega_2}{\omega_1} \right] \left(\frac{D}{D_{\mathrm{M}}} \right) \left[\frac{b}{d+b} \right] \frac{h+b+bD/(2D_{\mathrm{M}})}{h+bD/(2D_{\mathrm{M}})} \tag{23}$$

whose order of magnitude, obviously independent of the velocity, is around 0.2–0.3, the same as the ones we have adopted for the traditional geometries [14].

In the forced regimes the correction for the channel zone is less important. In particular, for the flow-rate forced regime, Eq. (17) can be assumed to be all-inclusive, also when referring to the whole length $(d+b)$

$$dN_{\mathrm{m}x,x=h} + bN'_{\mathrm{m}x,x=h} \approx \rho v h \omega_1 \tag{24}$$

$$Sh \approx \left[\frac{b}{d+b} \right] \left(\frac{vh}{D_{\mathrm{M}}} \right) = \left(\frac{h}{d} \right) \left[\frac{b}{d+b} \right] \left(\frac{D}{D_{\mathrm{M}}} \right) Pe\, y \tag{25}$$

Similarly, for the pellicular-forced regime, reference can be made to Eq. (19) in terms of the whole length $(d+b)$

$$dN_{\mathrm{m}x,x=h} + bN'_{\mathrm{m}x,x=h} \approx \rho \omega_1 \left[\frac{4Dv(d+b)}{\pi} \right]^{1/2} \tag{26}$$

$$Sh \approx \left[\frac{b}{d+b} \right] \left(\frac{D}{D_{\mathrm{M}}} \right) \left[4v \frac{d+b}{\pi D} \right]^{1/2}$$

$$\approx \left[\frac{4b^2}{\pi d(d+b)} \right]^{1/2} \left(\frac{D}{D_{\mathrm{M}}} \right) (Pe\, y)^{1/2} \tag{27}$$

Then, in these regimes, an increase in the velocity and Peclet numbers causes an increase in the Sherwood number, which can easily reach values of the order of unity or more, similar to the ones we have used for the interdigitated channel geometry [14].

By summarising, Eqs. (23), (25) and (27) we can demonstrate the dependence of Sh on $Pe\, y$ for the three limit regimes R1 (diffusive) (14), R2.1 (forced, flow-rate controlled) (16) and R2.2 (forced, pellicular) (18), respectively. Fig. 2 gives an example of these trends and shows that the regime is diffusive for low values of $Pe\, y$, controlled by the flow-rate for intermediate values of $Pe\, y$ and pellicular for high values of $Pe\, y$. For instance, by assuming, as in case (a) of Fig. 2:

$$b = d, \quad h = 0.1d, \quad D = 0.1D_{\mathrm{M}}, \quad \omega_1 = \omega_2 \tag{28}$$

we have

- R1:

$$(Pe\, y \ll 75), \quad Sh = 0.38 \tag{29}$$

- R2.1:

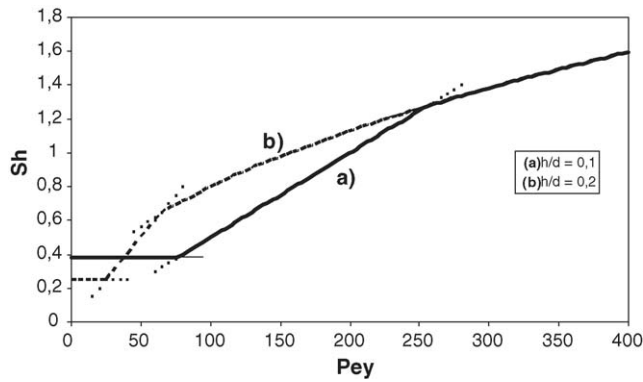$$(75 \ll Pe\, y \ll 250), \quad Sh = 0.005\, Pe\, y \tag{30}$$

Fig. 2. An example of the dependence of Sh on $Pe\,y$ for $\omega_1/\omega_2 = 1$; $D/D_M = 0.1$; $b/d = 1$; (a) $h/d = 0.1$; (b) $h/d = 0.2$.

- R2.2:

$$(Pe\,y \gg 250), \quad Sh = 0.08(Pe\,y)^{1/2} \tag{31}$$

and the range of $Pe\,y$ in which each regime is prevalent can easily be highlighted.

5. Traditional and non-traditional cells

The migration velocity v is directly connected to the mechanical driving force, that is the pressure difference between the beginning (channel 1) and the end (channel 2) of the domain migration path. As the pressure differences are low, the flow field can be assumed to be uniform and $h \ll b$; a simple integrated form of the Darcy equation for incompressible fluid is sufficient for a rather good evaluation of v

$$v = \frac{k(P_1 - P_2)}{\mu d} \tag{32}$$

By including this last equation in a detailed simulation tool, such as the one described in our previous work [14] the Peclet number and then the Sherwood number can be evaluated at each point of the plane of a cell and a more realistic consideration of the gas mass-transfer limitation can be taken into account. The final result, in terms of the characteristic curve, is a better prediction of the behaviour of the cell in the high current range and, in particular, a good a priori estimation of the limit current of the cell.

As a matter of fact, many of the differences between traditional and non-traditional cells can be interpreted in terms of gas mass-transfer limitations.

5.1. Traditional cells

In a traditional cell the channels are fed in parallel, so that no significant pressure difference can exist between two adjacent channels and the assumption of $v = 0$ is quite reasonable. So, a traditional cell should run under the diffusive regime R1 and should be characterised by a constant Sherwood number of the order of 0.2–0.4, according to the details of the geometry (h, d, b) and the permeability of the medium (D/D_M). A good fitting

of a traditional cell can be obtained by assuming a low constant Sherwood number [14].

5.2. Interdigitated cells

On the other hand, in interdigitated cells, there is a forced migration of the whole flow from the adduction channel to the adjacent outlet one. For medium–high current densities, the value of v is then of the order of 30–60 cm s^{-1}, with Peclet numbers of the order of 150–300 and Sherwood numbers of the order of 1.5–2. Flow-rate forced regimes are surely involved, so that the Sherwood number of the cell depends on v and then, at constant oxygen utilisation, increases as the cell current increases. The performance of the entire cell can be characterised using a Sherwood number that increases with the current or simply by a high constant Sh. At a low current, Sh has almost no influence, while at medium and high currents the assumption of a high, constant Sh is sufficient for a good simulation [14]. The advantages of interdigitated cells in terms of mass transfer resistances are evident, but the details of the dependence of Sh on $Pe\,y$ remain, to some extent, difficult to demonstrate.

5.3. Serpentine cells

More information can be obtained by considering the serpentine geometry and the experimental results obtained by the laboratories of the Italian National Agency for New Technologies, Energy and the Environment (ENEA) [16]. In a serpentine channel, the pressure difference between two adjacent counter current portions is related to the head losses through the channel
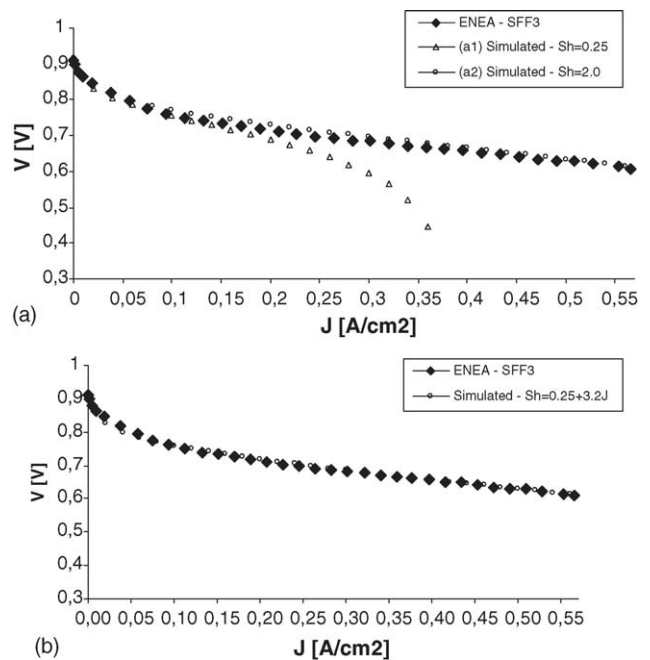

Fig. 3. An example of the fitting of the characteristic curve of a serpentine three-channel PEMFC. Data from [16]. The Sherwood numbers used for the various fitting attempts are: (a1) low, constant; (a2) high, constant; (b) increasing with the cell current.
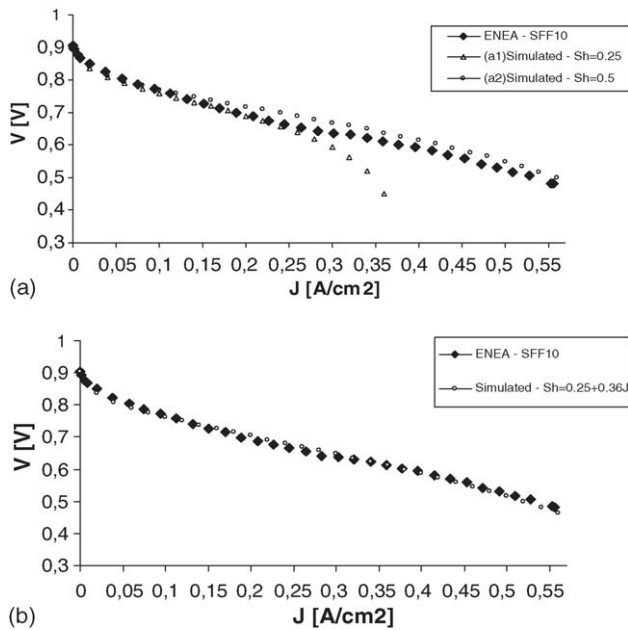
Fig. 4. An example of the fitting of the characteristic curve of a serpentine 10-channel PEMFC. Data from [16]. The Sherwood numbers used for the various fitting attempts are: (a1) low, constant; (a2) medium, constant; (b) increasing with the cell current.

itself; at this pressure difference only a fraction of the whole flow-rate is bypassed as a migration flow, so that the values of v are lower than in interdigitated cells. The number of parallel channels in the serpentine arrangement is also important. In a serpentine arrangement with many channels the head losses are lower; moreover, only the external channels are free to exchange mass by migration, so that the global effect is even lower.

These considerations are well illustrated by Figs. 3 and 4. In Fig. 3 a three-channel serpentine cell is considered: in such a system, a high Sh, strongly dependent on current, can be predicted from the estimate of v. In fact, the fitting is already good when a high constant Sh is assumed, but some improvement is also evident when reference is made to an Sh increasing with the current.

The effect is more evident in Fig. 4, where a 10-channel serpentine cell is considered. Medium values of Sh are to be used, and the assumption of a Sh that increases with the current yields a quite appreciable improvement in the fit.

6. Conclusions

In this work the relevance of the mass transfer of oxygen at PEMFC cathodes is stressed and a straightforward discussion of the interaction between diffusion and forced migration is presented in terms of limit regimes. Three limit regimes are determinable according to the values assumed by the Peclet number:

- R1, a diffusive regime in which the diffusion is controlling and the effect of migration is negligible;

- R2.1, a flow-rate controlled regime in which the velocity of migration is the only controlling parameter;
- R2.2, a pellicular-forced regime in which only a fraction of the forced flow, determined by diffusion, is effective.

For each regime the mass transfer can be characterised in terms of Sherwood number and a particular function $Sh(Pe\,y)$ by means of which the Sherwood number can be calculated from the Peclet number.

The results of this approach are then used in the discussion of the performance of different geometric arrangements, such as traditional, interdigitated and serpentine cells. As traditional cells appear to be characterised by a low constant Sh, their diffusive limitations can be overcome by using the interdigitated configuration where a much higher Sh is attained. Serpentine cells are characterised by intermediate values of Sh, depending on the number of channels, and show a more evident dependence on the cell current.

A more complete comparison of the various types of cell also requires the explicit consideration of the pressure field on the plane of the cell or, at least, along a couple of adjacent channels. This question will be the argument of the second part of this work.

Acknowledgments

References

[1] D.M. Bernardi, M.W. Verbrugge, AIChE J. 37 (1991) 1151.
[2] T.F. Fuller, J. Newman, J. Electrochem. Soc. 140 (1993) 1218.
[3] T.V. Nguyen, R.E. White, J. Electrochem. Soc. 140 (1993) 2178.
[4] R. Mosdale, S. Srinivasan, Electrochim. Acta 40 (1995) 413.
[5] M. De Francesco, E. Arato, P. Costa, J. Power Sources 132 (2004) 127.
[6] A. Serrafero, E. Arato, P. Costa, Proc. H2-AGE: When, Where, Why, H2www, Pisa, Italy, May 2004, Chem. Eng. Trans. 4 (2004) 423–428 (Edit. Sauro Pierucci, AIDIC Servizi S.r.l., Milano).
[7] S.-H. Ge, B.-L. Yi, J. Power Sources 124 (2003) 1.
[8] D. Singh, D.M. Lu, N. Djilali, Int. J. Eng. Sci. 37 (1999) 431.
[9] J. Amphlett, R. Baumert, R. Mann, B. Peppley, P. Roberge, J. Electrochem. Soc. 142 (1995) 1.
[10] J. Amphlett, R. Baumert, R. Mann, B. Peppley, P. Roberge, J. Electrochem. Soc. 142 (1995) 9.
[11] R. Mann, J. Amphlett, M. Hooper, H. Jensen, B. Peppley, P. Roberge, J. Power Sources 66 (2000) 173.
[12] A. Kulikovsky, J. Divisek, A. Kornyshev, J. Electrochem. Soc. 146 (1999) 3981.
[13] A. Kulikovsky, J. Divisek, A. Kornyshev, J. Electrochem. Soc. 147 (2000) 953.
[14] A. Serrafero, E. Arato, P. Costa, J. Power Sources 145 (2) (2005) 470.
[15] U. Sukkee, C.Y. Wang, J. Power Sources 125 (2004) 40.
[16] K. Zhukovsky, A. Pozio, J. Power Sources 130 (2004) 95.
[17] P. Costamagna, Chem. Eng. Sci. 56 (2001) 323.
[18] R.B. Bird, E.N. Steward, E.N. Lighfoot, Transport Phenomena, Wiley, New York, 1960.